

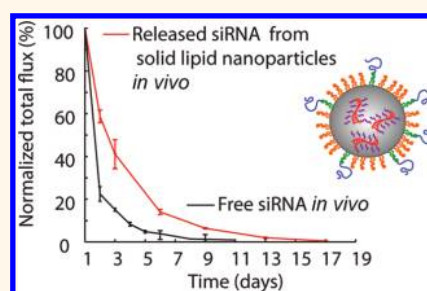
# In Vivo Sustained Release of siRNA from Solid Lipid Nanoparticles

Tatsiana Lobovkina,<sup>†</sup> Gunilla B. Jacobson,<sup>†</sup> Emilio Gonzalez-Gonzalez,<sup>\*,§</sup> Robyn P. Hickerson,<sup>‡</sup> Devin Leake,<sup>||</sup> Roger L. Kaspar,<sup>\*,‡</sup> Christopher H. Contag,<sup>\*,§,¶</sup> and Richard N. Zare<sup>†,\*</sup>

<sup>†</sup>Department of Chemistry, Stanford University, 333 Campus Drive, Stanford, California 94305-5080, United States, <sup>‡</sup>Department of Pediatrics, Stanford School of Medicine, Stanford, California 94305-5427, United States, <sup>§</sup>Molecular Imaging Program, Stanford University, Stanford, California 94305-5427, United States, <sup>‡</sup>TransDerm Inc., 2161 Delaware Avenue, Suite D, Santa Cruz, California 95060, United States, <sup>||</sup>Thermo Fisher Scientific, Dharmacon Products, 2650 Crescent Drive, Lafayette, Colorado 80026, United States, and <sup>¶</sup>Departments of Radiology, Microbiology, and Immunology, Stanford School of Medicine, Stanford, California 94305-5427, United States

Although small interfering RNAs (siRNAs) hold promise as nucleic-acid-based therapeutics, effective and well-controlled *in vivo* delivery remains challenging for two main reasons. First, crossing biological barriers such as the stratum corneum (for skin delivery), the cell membrane, and the endosomal compartment is difficult.<sup>1–5</sup> Second, long-term therapeutic effects will require repeated dosing. We already know that unmodified siRNA molecules are not taken up efficiently by most cells owing to their size ( $\sim 13\,000\ M_w$ ) and anionic nature and, therefore, may not result in effective gene silencing *in vivo*.<sup>6</sup> Nanoparticles have the potential for meeting both challenges. Utilization of nanoparticles engineered for slow, sustained, and controlled release of functional siRNA may decrease the frequency of treatment and lead to more effective therapies. To overcome the previously mentioned delivery challenges, lipid-based delivery systems, such as cationic liposomes and stable nucleic acid–lipid particle (SNALP), have been employed to mask the negative charges on the siRNA phosphodiester backbone and facilitate uptake.<sup>7–9</sup> Building on this theme, other delivery vehicles based on the variety of cationic and biodegradable polymers have been developed.<sup>10–15</sup> Many proposed approaches have demonstrated limited delivery of siRNA, and this research has revealed a need for combination strategies and new formulations. For this reason, a combinatorial synthesis of more than a thousand chemically diverse core–shell nanoparticles with cationic cores and variable shells was performed, and these were tested for intracellular siRNA and pDNA delivery.<sup>16</sup> This study highlights a certain design criteria for future nanoparticle development.

## ABSTRACT



Small interfering RNA (siRNA) is a highly potent drug in gene-based therapy with a challenge of being delivered in a sustained manner. Nanoparticle drug delivery systems allow for incorporating and controlled release of therapeutic payloads. We demonstrate that solid lipid nanoparticles can incorporate and provide sustained release of siRNA. Tristearin solid lipid nanoparticles, made by nanoprecipitation, were loaded with siRNA (4.4–5.5 wt % loading ratio) using a hydrophobic ion pairing approach that employs the cationic lipid DOTAP. Intradermal injection of these nanocarriers in mouse footpads resulted in prolonged siRNA release over a period of 10–13 days. *In vitro* cell studies showed that the released siRNA retained its activity. Nanoparticles developed in this study offer an alternative approach to polymeric nanoparticles for encapsulation and sustained delivery of siRNA with the advantage of being prepared from physiologically well-tolerated materials.

**KEYWORDS:** solid lipid nanoparticles · siRNA · sustained release · drug delivery

In general, nanoparticle delivery tools (lipid- and polymer-based) also require targeting moieties, such as antibodies, aptamers, and small peptides for directed delivery and improved specificity.<sup>11,12</sup>

As to the second challenge, sustained release of siRNA is highly desirable for many therapeutic applications, for example, where frequent siRNA injections are painful or high doses of intracellular siRNA levels are associated with toxicity.<sup>17,18</sup> Nanoparticles have already been engineered to act as a depot, resulting in slow, sustained, and

\* Address correspondence to zare@stanford.edu.

Received for review September 30, 2011 and accepted November 12, 2011.

Published online November 12, 2011  
10.1021/nn203745n

© 2011 American Chemical Society

targeted release of drugs, including siRNA.<sup>19–23</sup> The majority of biodegradable formulations that have provided sustained release of siRNA have employed polymeric materials in which siRNA is incorporated in a polymer core.<sup>19–23</sup> Alternatively, a modern class of biodegradable solid lipid nanoparticles (SLNPs), prepared from lipids that remain solid at body temperature, have been developed.<sup>24–27</sup> SLNPs have been used to incorporate various drugs, as well as imaging agents with the benefits of using physiological and nontoxic lipids.<sup>24,27–30</sup> Despite its many advantages, this type of nanoparticle remains largely unexplored for sustained oligonucleotide delivery. The hydrophobic nature of SLNPs impedes efficient loading of hydrophilic drugs, such as oligonucleotides. For protein- and peptide-loaded SLNPs, this challenge has partially been resolved by making peptide–surfactant conjugates prior to loading into SLNPs, which results in prolonged payload release.<sup>28,29</sup>

In this paper, we make a step toward using SLNPs for sustained siRNA delivery. We show that SLNPs can be loaded with siRNA by using a hydrophobic ion pairing (HIP) approach. The HIP we use consists of a tight complex of siRNA and a cationic lipid (DOTAP), allowing for efficient siRNA incorporation into the SLNP core. We demonstrate that prepared nanoparticles provide sustained release of siRNA *in vitro* and *in vivo* over a period of 10–13 days, with retained functionality.

## RESULTS AND DISCUSSION

Various solid lipids (such as tristearin, trilaurin, trimyristin, palmitic or stearic acids) and stabilizers (such as phospholipids, Pluronic F68, or Tween 80) have been employed to form SLNPs.<sup>24,27,28</sup> A number of reports describe applications of SLNPs for siRNA or DNA delivery.<sup>31–34</sup> In these studies, however, SLNPs are usually formed prior to binding of the oligonucleotides on the surface of the nanoparticle (NP), with no sustained *in vivo* release reported.<sup>31–34</sup> Solid lipids are hydrophobic molecules, which have little interaction with charged molecular species, whereas siRNAs are hydrophilic, negatively charged molecules. Such a difference in the properties between siRNA and solid lipids makes it difficult to incorporate oligonucleotides in the core of the SLNPs. To our knowledge, only one previous report exists where siRNAs, complexed with cationic polymer and dispersed in oil phase, were encapsulated in a solid lipid core.<sup>26</sup>

One way to overcome a challenge of loading SLNPs with oligonucleotides is to use a hydrophobic ion pairing (HIP) approach.<sup>19,20,35</sup> HIP is a technique in which a drug–surfactant complex is formed. This complex increases the lipophilicity of the drug and allows for incorporation of the drug in the lipid core of SLNP. In this study, we use a modified Bligh–Dyer method to form an HIP.<sup>36</sup> Briefly, a single-phase solution, consisting

of chloroform/methanol/water (CHF/MeOH/H<sub>2</sub>O, in the volume ratio of 1:2.2:1), is prepared. To this solution were added siRNA and a cationic lipid DOTAP in a 1:1 charge ratio, that is, one DOTAP molecule per phosphate group on the siRNA. In this mixture, DOTAP binds to siRNA and forms an HIP. The siRNA/DOTAP complex is tightly held together by electrostatic interaction between the negatively charged phosphodiester backbone and the positively charged DOTAP headgroup, while the DOTAP hydrophobic domains facilitate efficient encapsulation of the siRNA/DOTAP complex in the lipid nanoparticle.<sup>20</sup>

To prepare SLNPs, we use a nanoprecipitation/solvent displacement technique, which is similar to production of polymer nanoparticles and which has been used for preparing SLNPs.<sup>33,34,37,38</sup> First, lipids such as lecithin and DSPE-PEG were dissolved in a water/methanol (H<sub>2</sub>O/MeOH) receiver solution and preheated to 65 °C under gentle stirring. After the temperature was decreased to 35–40 °C, the siRNA/DOTAP complex in the CHF/MeOH/H<sub>2</sub>O was added to the receiver solution (Figure 1a–c, Feed solution 1). Next, a CHF solution of solid lipids was added to the receiver solution (Figure 1a–c, Feed solution 2).

Alternatively, the siRNA/DOTAP complex was extracted in CHF solution by phase separation and then dried until the CHF and water residues were evaporated. The dried siRNA/DOTAP complex was easily solubilized by CHF, mixed with solid lipids, and then added to the receiver solution (Figure 1b,d).

After all of the ingredients were added to the receiver solution, organic solvents were allowed to evaporate for 4–12 h under stirring, leading to nanoparticle precipitation. Occasionally, the solution was sonicated for 30 s to reduce nanoparticle agglomeration. Finally, the remaining organic solvents were removed by rotary evaporation, along with some of the water in order to obtain the desired final volume.

During the precipitation process, phospholipids were allowed to self-assemble on the nanoparticle surface with the hydrophobic hydrocarbon chains facing the solid lipid core, with the hydrophilic lipid headgroups and PEG moieties facing the aqueous environment (Figure 1e). Coating SLNPs and polymer NPs with phospholipids and PEGylated lipids is a common approach,<sup>30,37</sup> which has several advantages. Lipids and PEG moieties on the nanoparticle surface are used to stabilize nanoparticle dispersion; moreover, PEGylated NPs have prolonged circulation times *in vivo*, as well as reduced immunogenicity.<sup>39</sup>

The resulting SLNPs have diameters of ~150 nm as determined by scanning electron microscopy (SEM, Figure 2a). Dynamic light scattering measurements indicate some degree of agglomeration, with the main peak size ranging from 255 to 615 nm. The zeta potential of the nanoparticles is –20 mV in dilute phosphate buffer solution (PBS).

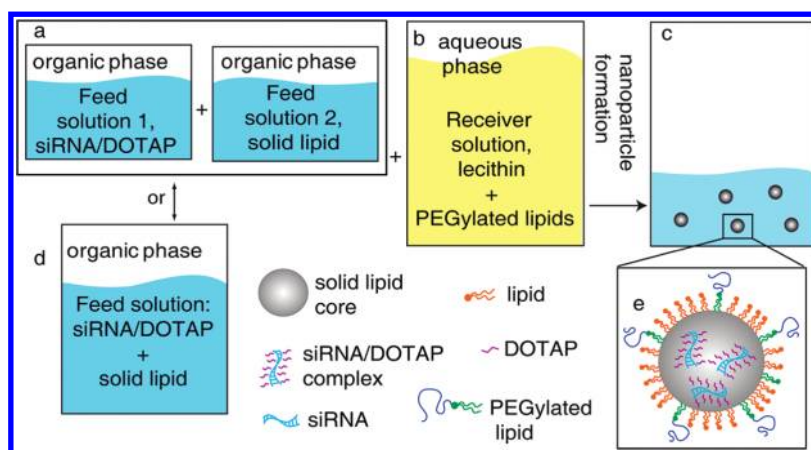


**Figure 1.** Schematic drawing showing preparation of SLNPs with encapsulated siRNA molecules. Feed solutions 1 and 2 pictured in (a) are sequentially added to the receiver solution pictured in (b). SLNPs form following evaporation of organic solvents, as shown in (c). Alternatively, siRNA/DOTAP complex and tristearin are solubilized in CHF, as shown in (d), and then added to the aqueous receiver solution. A schematic drawing of SLNP is presented in (e). The sizes and ratios of components are not to scale for illustrative purposes.

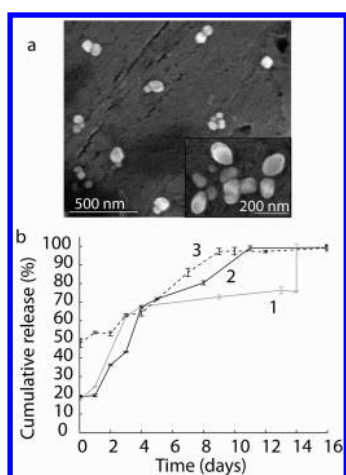


**Figure 2.** SLNP characterization. (a) SEM images of SLNPs. (b) Cumulative release rate of siRNA from SLNPs. Line 1, 5.5 wt % of K6a\_513a.12 siRNA; during the NP preparation the receiver solution contained an additional 0.5 wt % of PF 68, which had no effect on NP size. Line 2, 4.4 wt % of Accell CBL3 siRNA, and line 3, 4.8 wt % of K6a\_513a.12 siRNA.

Sustained release of siRNA from SLNPs in PBS (pH 7.4) containing surfactant Pluronic F68 (1 wt %) was determined by measuring the concentration of siRNA over time using the fluorescent dye SYBRGold (Figure 2b), as described in the Experimental Section. The surfactant PF68 was added to help disperse the SLNPs. In Figure 2b, SLNPs corresponding to lines 1 and 2 have been prepared according to the scheme shown in Figure 1a–c with a DSPE-PEG/lecithin/tristearin mass ratio of 0.1:0.2:1. The siRNA encapsulation ratio is 5.5 wt % in line 1 and 4.4 wt % in line 2.

The initial siRNA burst (*i.e.*, the amount of unencapsulated siRNA) is 17 and 22% in curves 1 and 2, respectively. We also observed that a certain amount of siRNA remained unreleased from SLNPs. To determine this amount, we dried the remaining nanoparticles and dissolved them in CHF solution. Next, a known

amount of water was added to CHF, and siRNA was extracted into the aqueous phase.

The siRNA concentration in water was measured as described above. The last data point in line 1 shows an example of such a measurement. Despite the observation that some siRNA remains unreleased *in vitro*, the *in vivo* degradation of SLNPs and release of siRNA may be facilitated by lipases present in a physiological milieu.<sup>26</sup> SLNPs with the release rate shown in Figure 2b, line 3, were prepared by combining the siRNA/DOTAP complex and solid lipids in the same CHF solution with a mass ratio of DSPE-PEG/lecithin/tristearin of 0.2:0.5:1 and a siRNA encapsulation ratio of 4.8 wt %. Such a nanoparticle preparation gives a higher initial burst of siRNA (up to 50%). For *in vivo* testing, we used the NP preparation scheme shown in Figure 1a–c.

To determine the *in vivo* release rate of siRNA, we injected a solution of SLNPs containing a fluorescently labeled siRNA mimic (siGLO Red), as well as unencapsulated siGLO Red at intradermal (ID) sites in footpads of mice. Intradermal injection of the nanoparticles allows for facile *in vivo* imaging due to the proximity of the SLNPs to the skin surface. *In vivo* red fluorescence signal was measured using an IVIS 200 imaging system as described in the Experimental Section. SLNPs were prepared with 5 and 4.4 wt % of siGLO Red and a total dose of 4 and 8  $\mu\text{g}$ —dashed and solid red lines in Figure 3a, respectively. Each dose was administered to a different group of mice. The lecithin/DSPE-PEG/tristearin mass ratio was 0.5:0.1:1 for the dashed line and 0.2:0.1:1 for the solid line. Despite the slight difference in SLNP formulation, the *in vivo* release curves of siGLO Red look similar. Figure 3 shows the decrease in fluorescence over time, with a faster decrease in signal for unencapsulated siGLO Red. During the first 24 h, the fluorescence intensity of unencapsulated siRNA decreases by 80%, versus 42–60% for

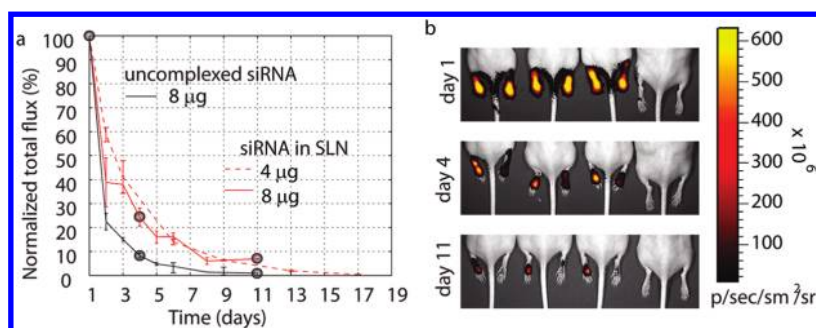


**Figure 3.** *In vivo* siRNA release data. (a) Normalized total flux versus time shows *in vivo* release of unencapsulated siGLO Red (black solid line) and siGLO Red encapsulated in SLNPs (red lines). Solid lines were obtained from a cohort of mice ( $n = 3$ ) by injecting siGLO Red SLNPs into the left paws and unencapsulated siGLO Red into right paws. (b) siGLO Red fluorescence signal collected from mouse paws injected with  $8 \mu\text{g}$  of siGLO Red. Images correspond to the data points from the solid red and black lines in (a), which are indicated with circles. The mouse on the right is a negative control with no siRNA or SLNP injected. Scale bar units are photons per second per  $\text{cm}^2$  per steradian.

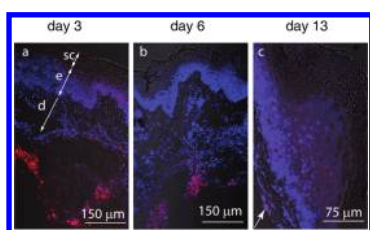


**Figure 4.** Fluorescence microscopy of skin sections prepared from mice treated with siGLO Red nanoparticles. (a–c) Images from frozen skin sections that were prepared from footpads treated by intradermal injection of siGLO Red SLNPs (the dose of siGLO Red is  $8 \mu\text{g}$ ) for 3, 6, or 13 days. Red, siGLO Red; blue, Syto-62 stained nuclei and cytoplasm. Stratum corneum (sc), epidermis (e), and dermis (d).

siGLO Red SLNPs, as shown in Figure 3a. Changes in fluorescence intensity for unencapsulated siRNA mirror our previous results, where doses of 2 and  $10 \mu\text{g}$  in  $50 \mu\text{L}$  of unencapsulated siRNA were intradermally injected into the mice footpads.<sup>20</sup> During the following 13 days, we observed a rapid decrease in fluorescence intensity for unencapsulated siGLO Red versus sustained release of siGLO Red from SLNPs. The observed *in vivo* dynamics mimic the *in vitro* release of siRNA (Figure 2b) in PBS solution.

In the *in vitro* experiments, siRNAs were released over the period of 9–10 days, and in the *in vivo* experiments, the siGLO Red signal decreased over the period of 10–13 days. Figure 3b shows images of mouse paws with siGLO Red fluorescence collected on day 1 (immediately following the initial injection), day 4, and day 11 (left paws, siGLO Red SLNPs; right paws, unencapsulated siGLO Red). The image, taken on day 1 in Figure 3b, corresponds to the data point marked with the circle at day 1 in Figure 3a. Both paws in Figure 3b at day 1 show high fluorescence signal. Images taken on days 4 and 11 in Figure 3b correspond to the data points marked with the circles on days 4 and 11 in Figure 3a (red solid line is for siGLO Red SLNP, and black line is for unencapsulated siGLO Red). The observed difference in fluorescence intensities between unencapsulated siGLO Red and siGLO Red

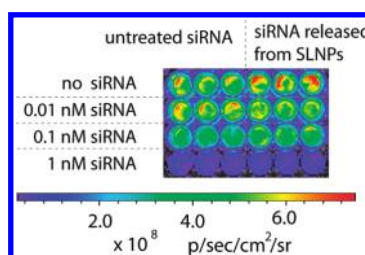


**Figure 5.** siRNA recovered from SLNPs has similar activity to unformulated input siRNA. Human 293FT cells were co-transfected in triplicate with pTD138 (a plasmid that expresses click beetle luciferase CBL<sup>17</sup>) and 0.01 to 1 nM unprocessed siRNA or siRNA released from SLNPs siRNAs as indicated. Luciferin was added 48 h post-transfection, and bioluminescence was visualized by using a Luminal I imaging system (Xenogen product from Caliper LifeSciences).

SLNPs confirms the sustained release of siGLO Red from SLNPs.

Additionally, confocal fluorescence microscopy was used to analyze the distribution of siGLO Red SLNPs in frozen skin sections prepared from footpads obtained from a separate group of mice that were treated in a similar fashion to those shown in Figure 3. Fluorescence microscopy (Figure 4) confirmed the presence of the siGLO Red SLNPs in the skin sections in the time period up to 13 days. On day 3, siRNA signal is detected in both the epidermis and dermis (Figure 4a). On day 6, the majority of siRNA is observed in the dermis (Figure 4b). Similarly, on day 13, the remaining siGLO Red signal is in the dermis (Figure 4c).

In order to verify that siRNA released from SLNPs retains functional activity, siRNA released from SLNPs was collected after a 7 day incubation at  $37^\circ\text{C}$  and analyzed for functional activity in transfected human 293FT cells. The results show that siRNA packaged in SLNPs retain the same functional activity as the original input siRNA (Figure 5).

## CONCLUSION

In summary, solid lipid nanoparticles were developed that allow for sustained *in vivo* siRNA delivery.

Nanoparticles were loaded with siRNA molecules by using a hydrophobic ion pairing approach in which functional siRNA activity was retained. Ion pairs consisted of siRNA and cationic lipid DOTAP, which allowed for efficient siRNA incorporation in the hydrophobic core of SLNP. The *in vivo* experiments demonstrate that SLNPs provide sustained release of siRNA in the period 10–13 days followed by the

intradermal injection of the nanoparticles. SLNPs may act as a sustained release system to prolong *in vivo* siRNA delivery and thus may control gene expression over time. Additionally, SLNPs provide an advantage of being prepared from physiological lipids with excellent biocompatibility, minimal toxicity, and they are less costly compared to polymeric carriers.

## EXPERIMENTAL SECTION

**Materials.** Analytical grade methanol, chloroform, molecular grade RNase-free water, and PBS (pH 7.4) were obtained from Fisher Scientific (Pittsburgh, PA). Tristearin was from Sigma Aldrich (St. Louis, MO), DOTAP (1,2-dioleoyl-3-trimethylammonium-propane); soybean lecithin (L- $\alpha$ -phosphatidylcholine) and DSPE-PEG (1,2-dioleoyl-*sn*-glycero-3-phosphoethanolamine-*N*-(methoxy(polyethylene glycol)-2000) were from Avanti Polar Lipids (Alabaster, AL), and SYBRGold was from Invitrogen (Carlsbad, CA). The K6a\_513a.12 siRNA<sup>40</sup> and Accell CBL3 siRNA for the *in vitro* release study and siGLO Red (DY-547) for the *in vivo* experiments were provided by Thermo Fisher Scientific, Dharmacon Products (Lafayette, CO).

**Synthesis of the Nanoparticles.** Lecithin and DSPE-PEG, dissolved in a 1:2 water/methanol solution with addition of 0.5% of 1-butanol as a cosurfactant (typical volume 9–18 mL with lipid concentration 15–100  $\mu\text{g/mL}$ ), were preheated to 65 °C under gentle stirring (receiver solution). After the temperature was decreased to 35–40 °C, the siRNA/DOTAP complex in the CHF/MeOH/H<sub>2</sub>O solution (total volume 840  $\mu\text{L}$ ) was added to the receiver solution. After that, tristearin (1 mg), dissolved in CHF at the concentration of 10 mg/mL, was added to the receiver solution. Alternatively, siRNA/DOTAP was extracted in CHF solution by phase separation, that is, addition of equal amounts of water and CHF. The siRNA/DOTAP complex in the CHF phase was then dried over a period of 8 h at room temperature until the CHF and water residues were evaporated. The dried siRNA/DOTAP complex was solubilized by CHF and mixed with solid lipids (500  $\mu\text{L}$  of total feed solution) and then added to the receiver solution. siRNA/DOTAP complex can also be stored at –20 °C for further use. The typical mixing mass ratio of siRNA/DOTAP/DSPE-PEG/lecithin/tristearin was 0.1:0.25:0.1–0.2:0.2–0.5:1. Organic solvents were allowed to evaporate for 4–12 h under stirring, leading to nanoparticle precipitation. During the precipitation process, the solution was sonicated for 30 s (PC3 Ultrasonics, bath sonicator at a frequency of 50 kHz). The remaining organic solvents were removed by rotary evaporation.

**Particle Analysis.** Scanning electron microscope (SEM) images were acquired using an FEI XL30 Sirion SEM with FEG source and EDX detector. Dilute aqueous nanoparticle solution was placed on SEM mount, and water was allowed to evaporate prior to SEM imaging. The hydrodynamic diameter and zeta-potential of the SLNPs were measured using a Malvern Zetasizer Nano ZS90. The zeta-potential of the nanoparticles was measured in phosphate-buffered saline solution (PBS, pH 7.4) diluted with water (1:20 dilution).

**Release Data.** Sustained release of siRNA (K6a\_513a.12 siRNA or Accell CBL3 siRNA) from SLNPs was performed by dispersing SLNPs in PBS solution (1% PF 68) in a typical volume of 10–15 mL. At each time interval, 500  $\mu\text{L}$  solution was removed and centrifuged for 5 min at 13 200 rpm to collect NPs.<sup>41</sup> The remaining SLNP solution was either replenished with a given amount of PBS solution or directly placed at 37 °C for further incubation. Then, 50  $\mu\text{L}$  of SYBRGold (1/500 dilution) was added to triplicate samples of 100  $\mu\text{L}$  of siRNA solution to measure fluorescence intensity, which was compared to a standard concentration curve. The encapsulation ratio was defined as  $100 \times (\text{siRNA mass})/(\text{total mass of the components used in the}$

NP preparation). For a typical NP preparation, on average, 50% of the initial amount of siRNA was detected by the release measurements, which indicates 50% encapsulation efficiency. This amount was defined as the maximum (100%) of cumulative release in Figure 2b. Each error bar represents the standard error.

**In Vivo Imaging.** Mouse paws (CD1 mice, Charles River, Hollister, CA) were imaged in an IVIS 200 imaging system (Xenogen product from Caliper LifeSciences) using the DsRed filter set (excitation at 460–490 and 500–550 nm; emissions at 575–650 nm). LivingImage software (Caliper LifeSciences) was used to quantify the resulting light emission, written as an overlay on Igor image analysis software (WaveMetrics, Inc.). DsRed background was subtracted, and raw values were reported as photons per second per cm<sup>2</sup> per steradian. For each siRNA dose (injection volume is 20–30  $\mu\text{L}$ ), a group of three mice was used for *in vivo* imaging. Error bars in Figure 3a are standard errors.

**Tissue Preparation and Imaging.** Skin sections were prepared by removing footpad skin from euthanized mice. Skin sections were embedded in OCT (Tissue-Tek, Torrance, CA) compound and frozen directly on dry ice. Skin cross sections were prepared, stained with Syto-62 fluorescent dye for nuclear and cytoplasmic staining, and mounted with Hydromount (National Diagnostic).

Microscopic visualization of tissue sections was performed using an upright Leica TCS SP2 AOBS confocal laser scanning microscope (Leica Microsystems, Wetzlar, Germany) equipped with HC PL FLUOTAR 20 $\times$  air objective. The 543 nm line of a He/Ne laser was used for excitation of siGLO RED, and the emission was collected by a photomultiplier tube at 565–623 nm. The 633 nm line of a He/Ne laser was used for excitation of Syto-62, and the emission was collected by a photomultiplier tube at 660–750 nm.

**In Vitro Assay.** Functional activity of CBL3 siRNA released from the SLNPs in PBS solution was compared to the untreated siRNA. SLNPs loaded with Accell CBL3 siRNA were prepared with an encapsulation ratio of 4.3 wt % (initial siRNA mass was 400  $\mu\text{g}$ ). Nanoparticles were dispersed in 2 mL of PBS (pH 7.4) and were incubated for 7 days at 37 °C to allow siRNA release. On day 7, the nanoparticle solution was filtered with 0.1  $\mu\text{m}$  centrifugal filter device (10 min at 13 200 rpm). After that, the nanoparticle suspension was concentrated with Amicon Ultra filter devices with the molecular weight cutoff of 3 kDa. This solution was further centrifuged for 10 min at 13 200 rpm to allow any NPs to settle. The top aqueous siRNA solution was collected and used for the *in vitro* study.

The siRNA functional activity was determined as described previously<sup>40</sup> with slight modifications. Briefly, 293FT cells were cotransfected (in triplicate) with a mixture of 40 ng of pTD138 expression plasmid,<sup>17</sup> 360 ng of pUC19 (as nucleic acid “filler”), Accell CBL3 siRNA (final concentration 0.01 to 1 nM per transfection), and K6a\_513a.12 siRNA (to give a final total siRNA concentration of 1 nM per transfection) diluted with 25  $\mu\text{L}$  in optiMEM medium (Invitrogen). One microliter of Lipofectamine 2000 was diluted in 25  $\mu\text{L}$  of optiMEM medium, added to the nucleic acid mixture, and incubated for 20 min at room temperature, prior to addition to the plated cells. After transfection (48 h), luciferin substrate (50  $\mu\text{L}$  of a 3 mg/mL solution) was

added, and the light emitted was visualized using the Xenogen Lumina II *in vivo* imaging system.

**Acknowledgment.** This work was supported by the National Science Foundation under CBET-0827806 and an NIH/NIAMS grant (RC2ARO58955) to R.L.K. and C.H.C. T.L. is the recipient of the Knut and Alice Wallenberg Foundation scholarship, Sweden. E.G.G. is the recipient of a PC Project fellowship.

## REFERENCES AND NOTES

- Juliano, R.; Bauman, J.; Kang, H.; Ming, X. Biological Barriers to Therapy with Antisense and siRNA Oligonucleotides. *Mol. Pharmaceutics* **2009**, *6*, 686–695.
- Gonzalez-Gonzalez, E.; Speaker, T. J.; Hickerson, R. P.; Spitler, R.; Flores, M. A.; Leake, D.; Contag, C. H.; Kaspar, R. L. Silencing of Reporter Gene Expression in Skin Using siRNAs and Expression of Plasmid DNA Delivered by a Soluble Protrusion Array Device (PAD). *Mol. Ther.* **2010**, *18*, 1667–1674.
- Li, C. X.; Parker, A.; Menocal, E.; Xiang, S. L.; Borodyansky, L.; Fruehauf, J. H. Delivery of RNA Interference. *Cell Cycle* **2006**, *5*, 2103–2109.
- Tokatlian, T.; Segura, T. siRNA Applications in Nanomedicine. *Wiley Interdiscip. Rev.: Nanomed. Nanobiotechnol.* **2010**, *2*, 305–315.
- Hickerson, R. P.; Vlassov, A. V.; Wang, Q.; Leake, D.; Ilves, H.; Gonzalez-Gonzalez, E.; Contag, C. H.; Johnston, B. H.; Kaspar, R. L. Stability Study of Unmodified siRNA and Relevance to Clinical Use. *Oligonucleotides* **2008**, *18*, 345–354.
- Dykxhoorn, D. M.; Lieberman, J. Knocking Down Disease with siRNAs. *Cell* **2006**, *126*, 231–235.
- Li, W. J.; Szoka, F. C. Lipid-Based Nanoparticles for Nucleic Acid Delivery. *Pharm. Res.* **2007**, *24*, 438–449.
- Whitehead, K. A.; Langer, R.; Anderson, D. G. Knocking Down Barriers: Advances in siRNA Delivery. *Nat. Rev. Drug Discovery* **2009**, *9*, 412–412.
- Kornek, M.; Lukacs-Kornek, V.; Limmer, A.; Raskopf, E.; Becker, U.; Kloeckner, M.; Sauerbruch, T.; Schmitz, V. 1,2-Dioleoyl-3-trimethylammonium-propane (DOTAP)-Formulated, Immune-Stimulatory Vascular Endothelial Growth Factor a Small Interfering RNA (siRNA) Increases Antitumoral Efficacy in Murine Orthotopic Hepatocellular. *Mol. Med.* **2008**, *14*, 365–373.
- Urban-Klein, B.; Werth, S.; Abuharbeid, S.; Czubayko, F.; Aigner, A. RNAi-Mediated Gene-Targeting through Systemic Application of Polyethylenimine (PEI)-Complexed siRNA *in Vivo*. *Gene Ther.* **2005**, *12*, 461–466.
- Davis, M. E.; Zuckerman, J. E.; Choi, C. H. J.; Seligson, D.; Tolcher, A.; Alabi, C. A.; Yen, Y.; Heidel, J. D.; Ribas, A. Evidence of RNAi in Humans from Systemically Administered siRNA *via* Targeted Nanoparticles. *Nature* **2010**, *464*, 1067–1070.
- Guo, P. X.; Coban, O.; Snead, N. M.; Trebley, J.; Hoeprich, S.; Guo, S. C.; Shu, Y. Engineering RNA for Targeted siRNA Delivery and Medical Application. *Adv. Drug Delivery Rev.* **2010**, *62*, 650–666.
- Tsutsumi, T.; Hirayama, F.; Uekama, K.; Arima, H. Potential Use of Polyamidoamine Dendrimer/ $\alpha$ -Cyclodextrin Conjugate (Generation 3, G3) as a Novel Carrier for Short Hairpin RNA-Expressing Plasmid DNA. *J. Pharm. Sci.* **2008**, *97*, 3022–3034.
- Han, H. D.; Mangala, L. S.; Lee, J. W.; Shahzad, M. M. K.; Kim, H. S.; Shen, D. Y.; Nam, E. J.; Mora, E. M.; Stone, R. L.; Lu, C. H.; *et al.* Targeted Gene Silencing Using RGD-Labeled Chitosan Nanoparticles. *Clin. Cancer Res.* **2010**, *16*, 3910–3922.
- Woodrow, K. A.; Cu, Y.; Booth, C. J.; Saucier-Sawyer, J. K.; Wood, M. J.; Saltzman, W. M. Intravaginal Gene Silencing Using Biodegradable Polymer Nanoparticles Densely Loaded with Small-Interfering RNA. *Nat. Mater.* **2009**, *8*, 526–533.
- Sieglwart, D. J.; Whitehead, K. A.; Nuhn, L.; Sahay, G.; Cheng, H.; Jiang, S.; Ma, M. L.; Lytton-Jean, A.; Vegas, A.; Fenton, P.; *et al.* Combinatorial Synthesis of Chemically Diverse Core–Shell Nanoparticles for Intracellular Delivery. *Proc. Natl. Acad. Sci. U.S.A.* **2011**, *108*, 12996–13001.
- Gonzalez-Gonzalez, E.; Ra, H.; Hickerson, R. P.; Wang, Q.; Piyawattanametha, W.; Mandella, M. J.; Kino, G. S.; Leake, D.; Avilion, A. A.; Solgaard, O.; Doyle, T. C.; *et al.* siRNA Silencing of Keratinocyte-Specific GFP Expression in a Transgenic Mouse Skin Model. *Gene Ther.* **2009**, *16*, 963–972.
- Judge, A.; Maclachlan, I. Overcoming the Innate Immune Response to Small Interfering RNA. *Hum. Gene Ther.* **2008**, *19*, 111–124.
- Lee, S.; Yang, S. C.; Kao, C.-Y.; Pierce, R. H.; Murthy, N. Solid Polymeric Microparticles Enhance the Delivery of siRNA to Macrophages *in Vivo*. *Nucleic Acids Res.* **2009**, *37*, e145.
- Jacobson, G. B.; Gonzalez-Gonzalez, E.; Spitler, R.; Shinde, R.; Leake, D.; Kaspar, R. L.; Contag, C. H.; Zare, R. N. Biodegradable Nanoparticles with Sustained Release of Functional siRNA in Skin. *J. Pharm. Sci.* **2010**, *99*, 4261–4266.
- Krebs, M. D.; Jeon, O.; Alsberg, E. Localized and Sustained Delivery of Silencing RNA from Macroscopic Biopolymer Hydrogels. *J. Am. Chem. Soc.* **2009**, *131*, 9204–9206.
- Patil, Y.; Panyam, J. Polymeric Nanoparticles for siRNA Delivery and Gene Silencing. *Int. J. Pharm.* **2009**, *367*, 195–203.
- Shi, J.; Xiao, Z.; Votruba, A. R.; Vilos, C.; Farokhzad, O. C. Differentially Charged Hollow Core/Shell Lipid–Polymer–wqLipid Hybrid Nanoparticles for Small Interfering RNA Delivery. *Angew. Chem., Int. Ed.* **2011**, *50*, 7027–31.
- Mehnert, W.; Mader, K. Solid Lipid Nanoparticles: Production, Characterization and Applications. *Adv. Drug Delivery Rev.* **2001**, *47*, 165–196.
- Jain, A.; Agarwal, A.; Majumder, S.; Lariya, N.; Khaya, A.; Agrawal, H.; Majumdar, S.; Agrawal, G. P. Mannosylated Solid Lipid Nanoparticles as Vectors for Site-Specific Delivery of an Anti-Cancer Drug. *J. Controlled Release* **2010**, *148*, 359–367.
- Xue, H. Y.; Wong, H. L. Tailoring Nanostructured Solid–Lipid Carriers for Time-Controlled Intracellular siRNA Kinetics To Sustain RNAi-Mediated Chemosensitization. *Biomaterials* **2011**, *32*, 2662–2672.
- Wissing, S. A.; Kayser, O.; Muller, R. H. Solid Lipid Nanoparticles for Parenteral Drug Delivery. *Adv. Drug Delivery Rev.* **2004**, *56*, 1257–1272.
- Almolda, A. J.; Souto, E. Solid Lipid Nanoparticles as a Drug Delivery System for Peptides and Proteins. *Adv. Drug Delivery Rev.* **2007**, *59*, 478–490.
- Gallarate, M.; Battaglia, L.; Peira, E.; Trotta, M. Peptide-Loaded Solid Lipid Nanoparticles Prepared through Coacervation Technique. *Int. J. Chem. Eng.* **2011**, *2011*, 1–6.
- Andreozzi, E.; Seo, J. W.; Ferrara, K.; Louie, A. Novel Method To Label Solid Lipid Nanoparticles with Cu-64 for Positron Emission Tomography Imaging. *Bioconjugate Chem.* **2011**, *22*, 808–818.
- Kim, H. R.; Kim, I. K.; Bae, K. H.; Lee, S. H.; Lee, Y.; Park, T. G. Cationic Solid Lipid Nanoparticles Reconstituted from Low Density Lipoprotein Components for Delivery of siRNA. *Mol. Pharmaceutics* **2008**, *5*, 622–631.
- Pedersen, N.; Hansen, S.; Heydenreich, A. V.; Kristensen, H. G.; Poulsen, H. S. Solid Lipid Nanoparticles Can Effectively Bind DNA, Streptavidin and Biotinylated Ligands. *Eur. J. Pharm. Biopharm.* **2006**, *62*, 155–162.
- Yu, W.; Liu, C.; Liu, Y.; Zhang, N.; Xu, W. Mannan-Modified Solid Lipid Nanoparticles for Targeted Gene Delivery to Alveolar Macrophages. *Pharm. Res.* **2010**, *27*, 1584–1596.
- Yu, W.; Liu, C.; Ye, J.; Zou, W.; Zhang, N.; Xu, W. Novel Cationic SLN Containing a Synthesized Single-Tailed Lipid as a Modifier for Gene Delivery. *Nanotechnology* **2009**, *20*, 215102.
- Patel, M. M.; Zeles, M. G.; Manning, M. C.; Randolph, T. W.; Anchordoquy, T. J. Degradation Kinetics of High Molecular Weight Poly(L-lactide) Microspheres and Release Mechanism of Lipid: DNA Complexes. *J. Pharm. Sci.* **2004**, *93*, 2573–2584.
- Bligh, E. G.; Dyer, W. J.; Rapid, A. Method of Total Lipid Extraction and Purification. *Can. J. Biochem. Physiol.* **1959**, *37*, 911–917.

37. Chan, J. M.; Zhang, L. F.; Yuet, K. P.; Liao, G.; Rhee, J. W.; Langer, R.; Farokhzad, O. C. PLGA-Lecithin-PEG Core–Shell Nanoparticles for Controlled Drug Delivery. *Biomaterials* **2009**, *30*, 1627–1634.
38. Zhang, S.; Yun, J.; Shen, S.; Chen, Z.; Yao, K.; Chen, J.; Chen, B. Formation of Solid Lipid Nanoparticles in a Microchannel System with a Cross-Shaped Junction. *Chem. Eng. Sci.* **2008**, *63*, 5600–5605.
39. Alexis, F.; Pridgen, E.; Molnar, L. K.; Farokhzad, O. C. Factors Affecting the Clearance and Biodistribution of Polymeric Nanoparticles. *Mol. Pharmaceutics* **2008**, *5*, 505–515.
40. Hickerson, R. P.; Smith, F. J. D.; Reeves, R. E.; Contag, C. H.; Leake, D.; Leachman, S. A.; Milstone, L. M.; McLean, W. H. I.; Kaspar, R. L. Single-Nucleotide-Specific siRNA Targeting in a Dominant-Negative Skin Model. *J. Invest. Dermatol.* **2008**, *128*, 594–605.
41. Ge, J.; Jacobson, G. B.; Lobovkina, T.; Holmberg, K.; Zare, R. N. Sustained Release of Nucleic Acids from Polymeric Nanoparticles Using Microemulsion Precipitation in Supercritical Carbon Dioxide. *Chem. Commun.* **2010**, *46*, 9034–9036.